SPACE TELESCOPE SCIENCE INSTITUTE
Operated for NASA by AURA

Instrument Science Report STIS 2015-02(v1)

Multi-Cycle Analysis of the STIS Dispersion Solutions

Paule Sonnentrucker[1]

[1]*Space Telescope Science Institute, Baltimore, MD*
September 25, 2015

ABSTRACT

The dispersion solutions for the most used STIS CCD and MAMA configurations are monitored on a yearly basis using two specific calibration programs. In this report, we present the analysis performed on the monitoring data obtained in Cycle 19, Cycle 20, and Cycle 21. Our comparison of the dispersion solution accuracies for the past three cycles indicates that the STIS dispersion solutions are remarkably stable and have not significantly changed since Cycle 17, the first cycle after STIS repair in 2009. For all modes monitored in these programs, the absolute scale (or zero-point) of the CCD dispersion solutions is accurate to within 0.2 pixels and the absolute scale of the MAMA dispersion solutions is accurate to within 0.1 pixels. The standard deviation around the zero-point (or relative wavelength scale) is less than 0.4 pixels for all CCD and MAMA configurations monitored over the past three cycles. As a result of such stability the wavelength calibration reference files for both the CCD and MAMA configurations have remained unchanged since Cycle 17. For the E230M configurations monitored in these programs, a clear non-linearity is present in the data which has the effect of artificially degrading the accuracy of the relative wavelength scales for these modes.

Contents

1. Introduction

The performance of all active instruments onboard HST is monitored every cycle through a variety of calibration programs. In this report, we describe how we monitor the accuracy of the dispersion solutions for the STIS/CCD and STIS/MAMA configurations that are most used by the astronomical community. Each cycle, the calibration programs designed to perform this monitoring are reviewed and tailored to the needs of the science community based on the most recent STIS usage statistics.

The STIS/CCD and STIS/MAMA dispersion solutions were initially derived on the ground using thermal vacuum data (Hulbert et al. 1997). The accuracy of all solutions was verified on-orbit during HST commissioning and was monitored every cycle until the STIS failure in 2004. After the repair of STIS in 2009, a new set of programs was executed to verify proper STIS operations and recalibrate the instrument. Programs 11858 (CCD) and 11859 (MAMA) were designed to check the dispersion solution accuracy for all STIS science modes offered to the community after the repair. These data showed that the accuracy of both the absolute wavelength scale (or zero-point) and the relative wavelength scale (or standard deviation around the zero-point) were consistent with those measured before the STIS failure for the CCD and MAMA modes monitored (Pascucci et al. 2011).

The analysis of the monitoring data obtained in subsequent Cycle 19, Cycle 20 and Cycle 21 is described in this report. The accuracies derived for both the absolute and relative wavelength scales are compared between cycles as well as with the mission requirements listed in Table 16.1 and Table 16.2 of the STIS Instrument Handbook.

2. Observations

Monitoring of the CCD and MAMA dispersion solutions occurs once per year in two different calibration programs. Both programs are typically scheduled in October to maintain the yearly cadence. Table 1 lists the program IDs, the dates of execution and the total number of orbits allocated to each program for Cycle 19, Cycle 20 and Cycle 21. All 6 programs executed successfully with no data loss. The dispersion solutions are verified using internal calibration lamp exposures for both the CCD and the MAMA detectors.

Table 1. Program Execution Summary

Cycle	PID	Detector	Observation Dates	Internal Orbit #
19	12768	CCD	10/17/2011	3
	12773	MAMA	10/17-18/2011	7
20	13137	CCD	10/15/2012	3
	13143	MAMA	10/18-19/2012	7
21	13540	CCD	10/28/2013	3
	13546	MAMA	10/28/1013	7

2.1 CCD Data

The CCD dispersion solutions were verified using internal wavecal exposures using the HITM1 and LINE lamps (TARGET=NONE). The 52x0.1" aperture was selected in all cases. The HITM1 lamp was chosen for most of the configurations using the G230LB, G230MB, G430L, G430M, G750L, G750M gratings due to this lamp's wider spatial illumination of the detector compared to the LINE lamp. The integration times were estimated based on HITM1 data from Cycle 17 in order to yield a S/N ratio of about 10 per pixel in row 900 after combining 32 rows. Adequate S/N is required at row 900 in order to support operations with the "E1" pseudo-apertures (Friedman 2005). The LINE lamp was used for the least sensitive of the CCD modes, the G430L/4300 setting, to yield a S/N ratio adequate to verify the dispersion solution with this configuration too. Table 2 lists the 16 STIS CCD configurations monitored over the past three cycles, the lamp used for each exposure as well as the integration time allocated to each exposure. This program structure was carried forward from Cycle 18 assuming no significant lamp degradation has occurred since that time.

Table 2. Monitoring Observations for the STIS/CCD in PID 12768 (Cycle 19), PID13137 (Cycle 20) and PID13540 (Cycle 21). All three programs adopted the same structure as in Cycle 18.

Spectral Element	Central Wavelength [Å]	Lamp type	Integration Time [s]
G230LB	2375	HITM1	220.0
G230MB	1713	HITM1	368.0
G230MB	1995	HITM1	190.0
G230MB	2416	HITM1	41.0
G230MB	2697	HITM1	14.0
G230MB	3115	HITM1	24.0
G430L	4300	LINE	10.0
G430M	3165	HITM1	10.0
G430M	3680	HITM1	10.0
G430M	4961	HITM1	24.0
G430M	5471	HITM1	26.0
G750L	7751	HITM1	6.2
G750M	5734	HITM1	5.9
G750M	6768	HITM1	3.9
G750M	8311	HITM1	10.0
G750M	9336	HITM1	10.0

2.2 MAMA Data

The MAMA data were also obtained using internal wavecals exposures (TARGET=NONE). The LINE lamp, the brightest of the three Pt/Cr-Ne lamps, was used for all MAMA configurations monitored in Cycle 19, Cycle 20 and Cycle 21 to yield S/N ratios adequate to sample enough emission lines in the wavelength ranges covered by each configuration. The integration times recommended by Ayres et al. (2008) and used in Cycles 17 and 18 were carried forward in Cycles 19, 20, and 21, under the assumption that there is no significant lamp degradation over time. Table 3 lists the 16 configurations monitored since Cycle 18 along with the apertures used and the adopted integration times.

Table 3. Monitoring Observations for the STIS/MAMA in PID 12773 (Cycle 19), PID13143 (Cycle 20) and PID13546 (Cycle 21). All programs adopted the same structure as in Cycle 18.

Spectral Element	**Central Wavelength [Å]**	**Aperture ["]**	**Integration Time [s]**
E140M	1425	0.2X0.06	663.2
E140H	1598	0.2X0.09	400.5
E140H	1271	0.2X0.09	400
E140H	1343	0.2X0.09	550
E230M	1978	0.2X0.06	190.3
E230M	2415	0.2X0.06	135
E230M	2561	0.2X0.06	120
E230M	2707	0.2X0.06	87.2
E230H	1763	0.1X0.09	800
E230H	1963	0.1X0.09	800.0
E230H	2713	0.1X0.09	500
G140M	1218	52X0.1	450
G140L	1425	52X0.1	140
G230M	1687	52X0.1	310
G230M	3055	52X0.1	22.0
G230L	2376	52X0.05	47.6

3. Data Reduction and Analysis

Wavecal observations are not calibrated by the CalSTIS pipeline. In order to produce the calibrated, 1-D extracted lamp spectra needed for the CCD and MAMA analyses, one needs to ingest the wavecal exposures into CalSTIS as if they were science exposures. To do so, each *raw* wavecal image (xxx_raw.fits) gets copied over into a companion wavecal image to create a new *wav* image (xxx_wav.fits) that will be invoked as argument in the WAVECAL header keyword. For each *raw* image, the argument in keyword ASN_MTYP then needs to be changed from WAVE to SCIENCE to force CalSTIS to calibrate the wavecal image as a science image. A number of additional header keywords in the *raw* image need modifications in order to calibrate the CCD and MAMA data adequately. Python scripts perform these calibration tasks automatically for the CCD and MAMA monitoring data. These scripts call the most recent version of CalSTIS along with all adequate reference files associated to each observation to generate 1-D extracted spectra (*xxx_x1d.fits*) for each observation. For the CCD verification, only the spectra extracted at the center of the detector (row 512) are considered here. For the MAMA echelle verification, order merging is required to produce 1-D spectra covering the full wavelength ranges under consideration here. The order merging is performed by simply interleaving the flux-wavelength points in ascending wavelength order.

The analysis is performed using a series of IDL subroutines developed locally and customized to the CCD and the MAMA observations (Pascucci et al. 2011). The analysis consists in comparing the wavelength of the emission lines measured in each *x1d* spectrum against the relevant laboratory wavelengths obtained from the compilations of Sansonetti et al. (2004) and Wallace and Hinkel (2009). Three methods were used to measure the peak of the spectral emission lines seen in the data.

1. Spk Method: Computes the difference (in pixels) between the laboratory lines and the peak of the observed emission lines in a range of 0.5 pixels around the expected centroid.
2. Gaussian Method: Fits a Gaussian to the observed emission lines and computes the difference between the Gaussian centroid and the laboratory lines
3. WeightSpK Method: Computes the observed emission line centroid weighted mean by using the counts over 2 pixels on each side of the line centroid as weights.

For each configuration, the fitted lines are inspected interactively and labeled as good = "yes" or "no". "Good" lines are those lines that show no sign of blending and are not saturated. The difference distribution between the laboratory lines and the observed lines is subsequently derived only for the subset of emission lines for which all three methods returned emission lines labeled as "good". For each method, the mean and standard deviation around the mean are computed and inter-compared.

4. Results

4.1 CCD Modes

For each grating, the difference distributions (or offsets) between the measured emission lines and the corresponding laboratory lines are calculated in units of pixels. The mean (Mean) and standard deviation (Std) using the Gaussian method are listed in Tables 4-6 (Appendix A.1). Only those lines labeled as "good" during the analysis are used to construct the difference distributions for all CCD modes monitored in the calibration programs executed in Cycles 19, 20 and 21. The 1-D spectra considered here are those corresponding to the center of the CCD detector (row 512).

Figures 1-3 below compare the difference distributions (or offsets) measured for the three cycles discussed here. The mean of each offset distribution represents a measure of the accuracy of the absolute dispersion solution or its zero-point. The standard deviation measures the accuracy of the relative wavelength scale over the entire wavelength range covered by a particular configuration. All cycles considered, the measurements show that the zero-point accuracy is typically smaller than 0.15 pixels for the G230 gratings (Figure 1), smaller than 0.11 pixels for the G430 gratings (Figure 2) and smaller than 0.13 pixels for the G750 gratings (Figure 3). The standard deviations are better than 0.35 pixels for all configurations expect G230MB/1713 where a standard deviation of 0.42 pixels is measured. This somewhat larger deviation is driven by the small number of emission lines available for the analysis (Figure 1).

This multi-cycle comparison shows that the dispersion solution accuracy for all 16 CCD modes monitored yearly is very stable. Since the repair of STIS in 2009, the variation in the accuracy of the relative wavelength scale is at most 20%. The variation in the accuracy of the absolute wavelength scale is typically of factor 2-3 but can amount to a factor of 10 for those modes that have poor emission line spectra (G230MB/1713) and thus have less well-constrained solutions. These variations are expected and are mostly caused by non-repeatability in the MSM motion and thermal drifts. The randomness of the measured variations further indicates that no systematic trends have developed over time. The requirements to have an absolute wavelength scale accuracy of about 0.2-0.5 pixels and a relative wavelength scale accuracy of about 0.1-0.4 pixels are clearly met for all CCD configurations monitored so far (see Section 4.3.2 and Table 16.1 of the STIS Data Handbook).

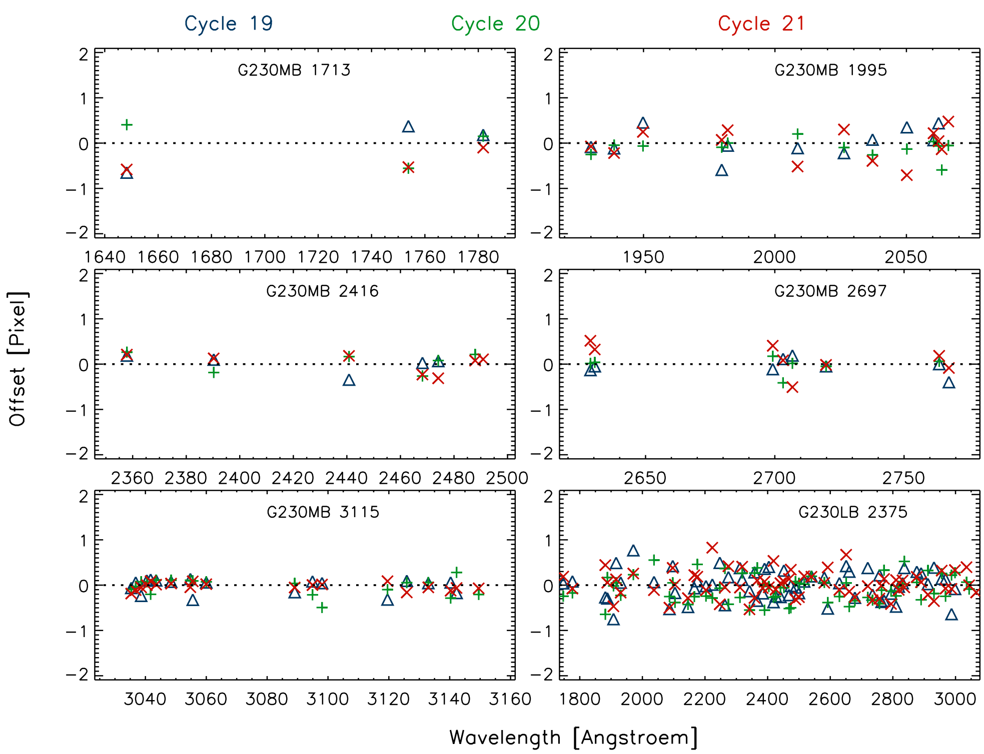

Figure 1: Difference (or offset) between fitted line centroids and corresponding laboratory wavelengths using the Gaussian fitting method for the emission lines observed with the STIS CCD G230 gratings. Cycle 19 measurements appear as blue symbols, Cycle 20 measurements appear as green symbols and Cycle 21 measurements appear as red symbols. One pixel corresponds to 175 km/s for the L grating and 20 km/s for the M grating.

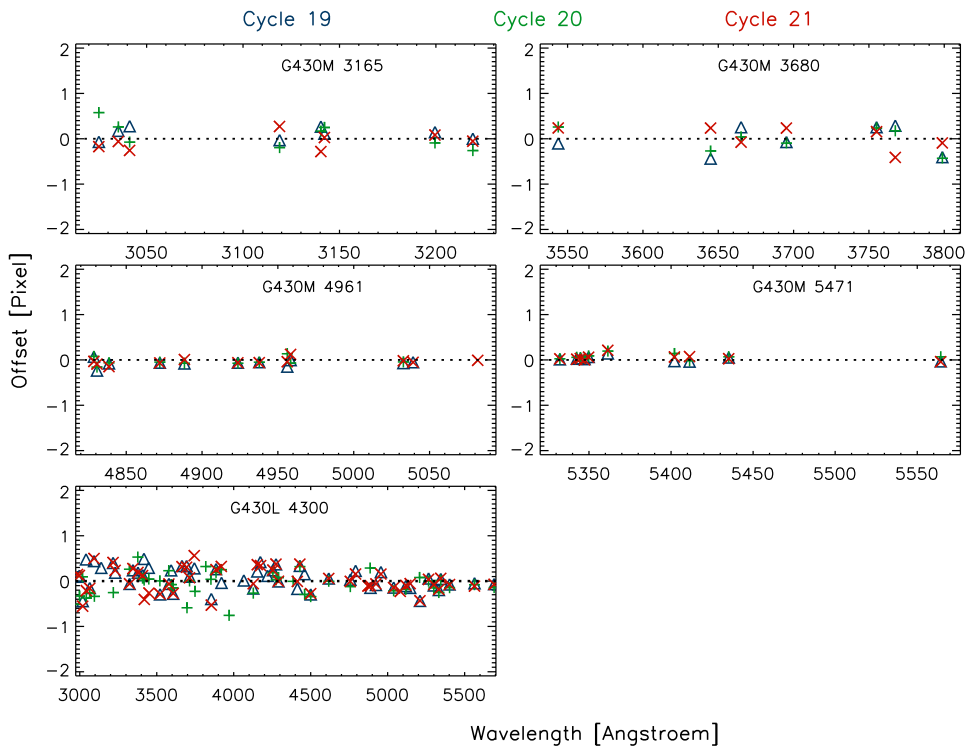

Figure 2: Difference (or offset) between fitted line centroids and corresponding laboratory wavelengths using the Gaussian fitting method for the emission lines observed with the STIS CCD G430 gratings. Cycle 19 measurements appear as blue symbols, Cycle 20 measurements appear as green symbols and Cycle 21 measurements appear as red symbols. One pixel corresponds to 240 km/s for the L grating and 25 km/s for the M grating.

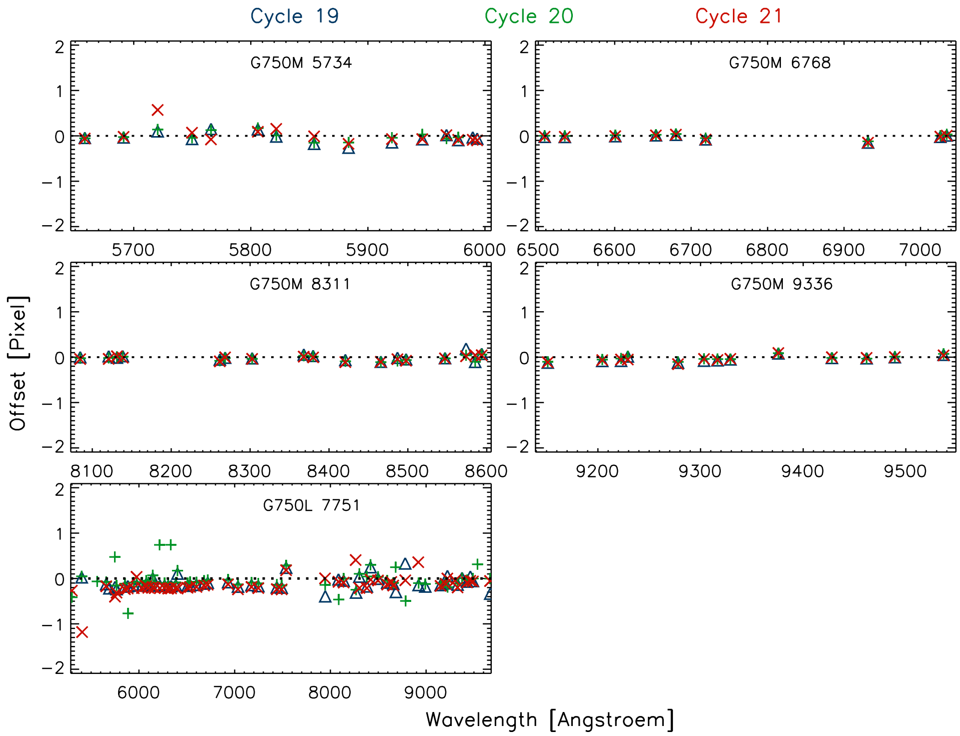

Figure 3: Difference (or offset) between fitted line centroids and corresponding laboratory wavelengths using the Gaussian fitting method for the emission lines observed with the STIS CCD G750 gratings. Cycle 19 measurements appear as blue symbols, Cycle 20 measurements appear as green symbols and Cycle 21 measurements appear as red symbols. One pixel corresponds to 197 km/s for the L grating and 22 km/s for the M grating.

4.2 MAMA Modes

For each grating, the difference distributions (or offsets) between the measured emission lines and the corresponding laboratory lines are calculated in units of pixels. The mean (Mean) and standard deviation (Std) using the Gaussian method are listed in Tables 7-9 (Appendix A.2). As before, only those lines labeled as "good" during the analysis are used to construct the difference distributions for all MAMA modes monitored in the calibration programs executed in Cycles 19, 20 and 21. The 1-D spectra used here are those resulting from order merging as described in Section 3.

Figures 4-6 below compare the difference distributions (or offsets) measured for all 16 configurations over the three cycles considered here. The mean of each offset distribution represents a measure of the accuracy of the absolute dispersion solution or its zero-point. The standard deviation measures the accuracy of the relative wavelength scale over the entire wavelength range covered by a particular configuration.

For the echelle gratings, the analysis shows that the E140 configurations exhibit offset distributions with a mean that is typically smaller than 0.13 pixels, resulting in an absolute wavelength scale accuracy better than ~0.17 km/s for the H grating and 0.43 km/s for the M grating (Figure 4). The accuracy of the relative wavelength scale is always smaller than 0.3 pixels, as required. For the E230 configurations, the accuracy of the absolute wavelength scale is always better than 0.2 pixels for both the H and M configurations (Figure 5). The accuracy of the relative wavelength scale is better than 0.3 pixels for the H configurations but can increase to as much as 0.45 pixels for the M configurations. Figure 5 clearly shows that non-linear residual trends are present for all E230M configurations monitored here; these trends produce an artificial degradation of the accuracy of the relative scales for these settings. Ayres (2010) indicated the presence of these trends and suggested applying modifications to the dispersion solutions to decrease the impact of these non-linearities on the data quality. Preliminary testing was performed by Pascucci et al. (2011) for some settings. The modification of the dispersion solution algorithm proposed by Ayres (2010) has not been implemented in CalSTIS to-date as comprehensive testing is still required to fully validate the proposed changes.

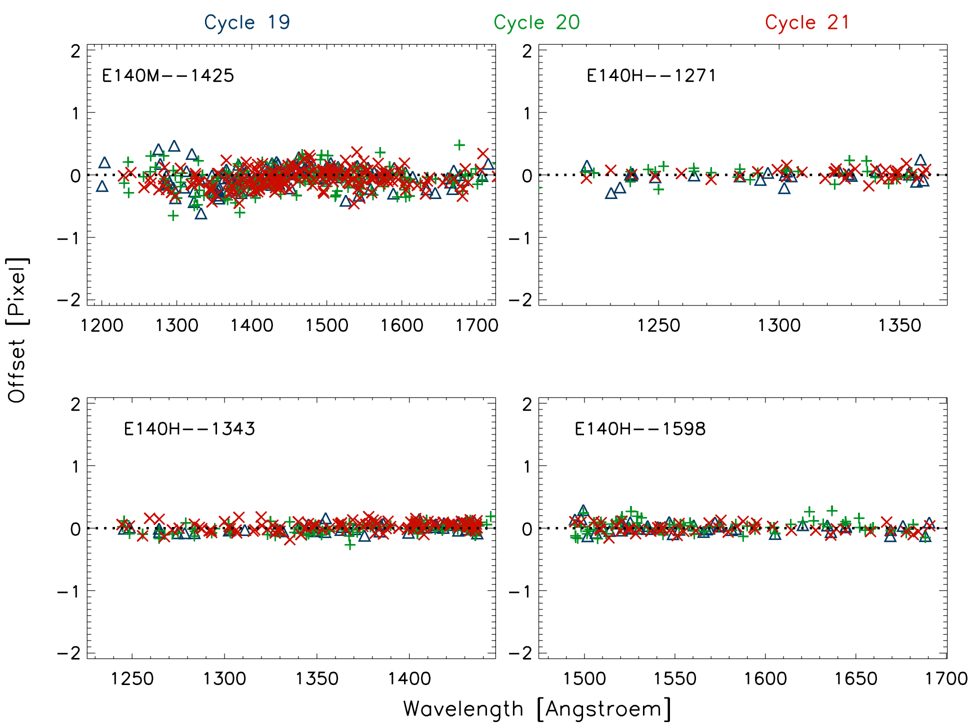

Figure 4: Difference (or offset) between fitted line centroids and corresponding laboratory wavelengths using the Gaussian fitting method for the emission lines observed with the STIS MAMA E140 gratings. Cycle 19 measurements appear as blue symbols, Cycle 20 measurements appear as green symbols and Cycle 21 measurements appear as red symbols. 1 pixel corresponds to 1.3 km/s for the H grating and 3.3 km/s for the M grating.

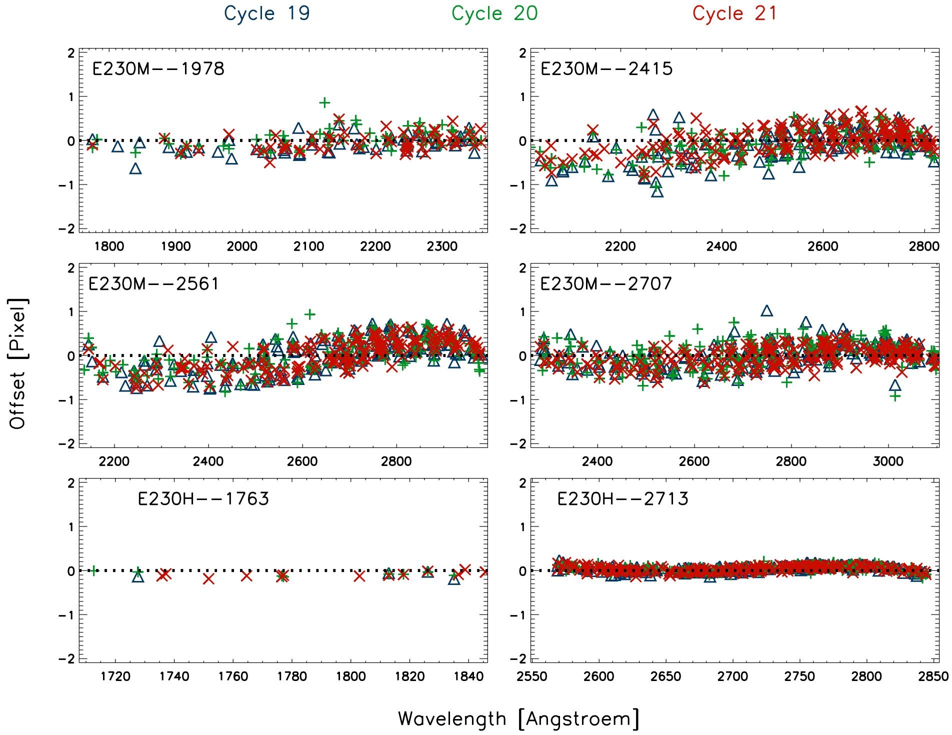

Figure 5: Difference (or offset) between fitted line centroids and corresponding laboratory wavelengths using the Gaussian fitting method for the emission lines observed with the STIS MAMA E230 gratings. Cycle 19 measurements appear as blue symbols, Cycle 20 measurements appear as green symbols and Cycle 21 measurements appear as red symbols. 1 pixel corresponds to 1.3 km/s for the H grating and 3.3 km/s for the M grating.

The mean of the offset distributions for the first-order G140 gratings are typically smaller than 0.14 pixels, indicating that the absolute wavelength scale is accurate to better than 18 km/s for the L grating and 1.7 km/s for the M grating (Figure 6). For the G230 gratings, the mean of the offset distributions is typically smaller than 0.11 pixels, leading to an absolute wavelength scale accuracy better than 22 km/s for the L grating and 1.8 km/s for the M grating (Figure 6). The accuracy of the relative wavelength scale is measured to be better than 0.2 pixels for all first-order gratings but the G140M/1218 and G130M/1687 where the more limited number of lines available for the analysis increase the uncertainty of the verification. This multi-cycle comparison shows that the STIS MAMA first-order dispersion solutions continue to be remakably stable over time. Since the repain of STIS, the variation in the accuracy of the absolute and relative wavelength scales are fully consistent with the mission requirements (Table 16.2 of the STIS Instrument Handbook).

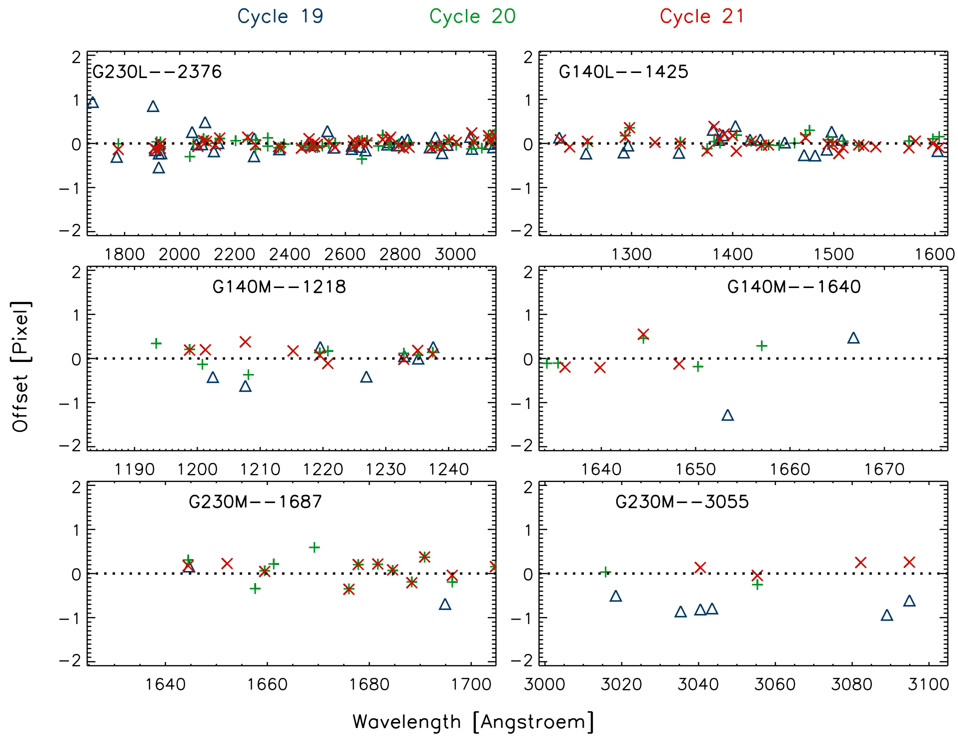

Figure 6: Difference (or offset) between fitted line centroids and corresponding laboratory wavelengths using the Gaussian fitting method for the emission lines observed with the STIS MAMA first-order gratings. Cycle 19 measurements appear as blue symbols, Cycle 20 measurements appear as green symbols and Cycle 21 measurements appear as red symbols. 1 pixel corresponds to 199 km/s for G230L, 16 km/s for G230M, 12 km/s for G140M and 126 km/s for G140L.

4. Summary

The accuracy of the on-orbit dispersion solutions for the most used STIS MAMA and CCD configurations is monitored every cycle as part of the general STIS calibration effort. A comparison of the data analysis for Cycles 19, 20 and 21 indicates that the dispersion solutions are very stable since the STIS repair in 2009. The wavelength solution absolute scale (or zero-point) accuracy is better than 0.2 pixels for all MAMA and CCD configurations monitored over these three cycles. For the CCD detectors, the relative wavelength scale accuracy is measured to be better than 0.2 pixels for the G230 and G430 gratings and better than 0.1 pixel for the G750 gratings. For the MAMA modes, the relative wavelength scale accuracy is measured to be better than 0.4 pixels for most gratings. The analysis presented here indicates that the accuracy of both the dispersion solution zero-points and the relative wavelength scales fully meet the mission requirements. As a result, updates to the wavelength scale references were not required since Cycle 17.

Recommendations: The yearly monitoring of the dispersion solution for the configurations most used with the STIS CCD and MAMA detectors should continue as part of the overall STIS calibration effort with the same observing cadence. Implementation of new terms in the current solutions should be considered in order to improve the relative accuracy of wavelength scale for the E230M configurations as already suggested by Ayres (2010) and Pascucci et al. (2011). The structure of the MAMA and CCD monitoring programs has remained unchanged since Cycle 18 under the assumption that the wavecal lamps have not faded significantly. The data analysis indicates that the exposure times listed in Table 1 are still adequate to perform the dispersion solution verifications described here for most modes in the next coming cycle. In the near future, one might want to verify the level of degradation that the lamp outputs have suffered with time since Cycle 17 and, if need be, adjust the observing structures accordingly.

References

Ayres, 2008, ApJS, 177, 626

Ayres, 2010, The 2010 STScI Calibration Workshop, page 57, "Ironing Out the Wrinkles in STIS"

Friedman, 2005, Instrument Science Report STIS 2005-03, "Wavelength Calibration Accuracy of the first-order CCD modes using the E1 position."

Hulbert et al., 1997, Instrument Science Report STIS 1997-02, "The STScI STIS Pipeline VII: Extraction of 1-D Spectra"

Pascucci et al., 2011, Instrument Science Report STIS 2011-01, "Wavelength Calibration Accuracy for the STIS CCD and MAMA Modes"

Sansonetti et al., 2004, ApJS, 153, 555

Wallace & Hinkle, 2009, ApJ, 700, 720

Appendix A

A.1 STIS CCD Configurations

Tables 4-6 report, for each setting, the mean (Mean) and standard deviation (Std) of the difference distribution (or offset) in units of pixels. The difference between the fitted line centroids and the corresponding laboratory wavelengths is calculated for all lamp lines identified with a value of "good" in the data, using the Gaussian method (see Section 3). One pixel corresponds to 175 km/s for G230LB, 20 km/s for G230MB, 240 km/s for G430L, 25 km/s for G430M, 197 km/s for G750L and 22 km/s for G750M. Figures 1-3 of Section 4.1 display these offsets versus wavelength for all 16 CCD configurations monitored during the there cycles considered here.

Table 4: CCD Dispersion Solution Verification for the G230 Gratings.

	Cycle 19	**Cycle 20**	**Cycle 21**
Grating-cenwave	**Mean (pixel)** **Std (pixel)**	**Mean (pixel)** **Std (pixel)**	**Mean (pixel)** **Std (pixel)**
G230LB - 2375	0.03 0.32	-0.07 0.27	0.01 0.28
G230MB - 1713	0.07 0.32	0.03 0.42	-0.30 0.31
- 1995	0.02 0.27	-0.09 0.16	-0.02 0.16
- 2416	0.01 0.22	0.05 0.23	0.03 0.22
- 2697	-0.05 0.20	-0.02 0.22	0.13 0.38
- 3115	-0.02 0.21	-0.05 0.28	-0.05 0.10

Table 5: CCD Dispersion Solution Verification for the G430 Gratings

	Cycle 19	**Cycle 20**	**Cycle 21**
Grating-cenwave	**Mean (pixel)** **Std (pixel)**	**Mean (pixel)** **Std (pixel)**	**Mean (pixel)** **Std (pixel)**
G430L - 4300	0.04 0.26	-0.07 0.28	0.01 0.28
G430M - 3165	0.10 0.11	0.03 0.22	-0.02 0.16
- 3680	-0.03 0.33	-0.02 0.27	0.04 0.27
- 4961	-0.10 0.11	-0.05 0.12	-0.05 0.09
- 5471	0.04 0.08	0.09 0.10	0.08 0.10

Table 6: CCD Dispersion Solution Verification for the G750 Gratings

	Cycle 19	Cycle 20	Cycle 21
Grating-cenwave	**Mean (pixel)** **Std (pixel)**	**Mean (pixel)** **Std (pixel)**	**Mean (pixel)** **Std (pixel)**
G750L - 7751	-0.10 0.14	-0.03 0.22	-0.12 0.16
G750M - 5734	-0.03 0.08	-0.00 0.07	0.01 0.13
- 6768	-0.02 0.04	-0.00 0.04	-0.02 0.04
- 8311	0.00 0.07	-0.03 0.05	-0.02 0.05
- 9336	-0.03 0.08	-0.01 0.07	-0.04 0.07

A.2 STIS MAMA Configurations

Tables 7-9 report, for each setting, the mean (Mean) and standard deviation (Std) of the difference distribution (or offset) in units of pixels. The difference between the fitted line centroids and the corresponding laboratory wavelengths is calculated for all lamp lines identified with a value of "good" in the data, using the Gaussian method (see Section 3). One pixel corresponds to 199 km/s for G230L, 16 km/s for G230M, 12 km/s for G140M and 126 km/s for G140L. For the echelle gratings, 1 pixel corresponds to 1.3 km/s for the high resolution (H) modes and to 3.3 km/s for the medium resolution (M) modes. Figures 4-6 of Section 4.2 display these offsets versus wavelength for all 16 MAMA configurations monitored during the there cycles considered here.

Table 7: Low Resolution MAMA First-Order Gratings

	Cycle 19	Cycle 20	Cycle 21
Grating-cenwave	**Mean (pixel)** **Std (pixel)**	**Mean (pixel)** **Std (pixel)**	**Mean (pixel)** **Std (pixel)**
G140L - 1425	0.01 0.21	0.07 0.11	0.02 0.14
G140M - 1218	-0.12 0.35	0.08 0.21	0.13 0.14
G230L - 2376	-0.04 0.16	-0.01 0.11	0.01 0.10
G230M - 1687	-0.26 0.59	0.05 0.25	0.04 0.19
- 3055	-0.75 0.16	-0.11 0.20	0.15 0.15

Table 8: Medium Resolution MAMA Echelle Gratings

	Cycle 19	Cycle 20	Cycle 21
Grating-cenwave	**Mean (pixel)** **Std (pixel)**	**Mean (pixel)** **Std (pixel)**	**Mean (pixel)** **Std (pixel)**
E140M - 1425	-0.04 0.18	-0.07 0.18	-0.06 0.15
E230M - 1978	-0.08 0.19	0.04 0.21	-0.04 0.19
- 2415	-0.07 0.44	-0.08 0.32	0.01 0.30
- 2561	0.06 0.39	0.05 0.34	0.04 0.33
- 2707	0.06 0.31	0.05 0.28	-0.02 0.22

Table 9: High Resolution MAMA Echelle Gratings

	Cycle 19	Cycle 20	Cycle 21
Grating-cenwave	**Mean (pixel)** **Std (pixel)**	**Mean (pixel)** **Std (pixel)**	**Mean (pixel)** **Std (pixel)**
E140H -1271	-0.04 0.28	-0.01 0.32	0.05 0.19
- 1343	0.04 0.16	-0.03 0.19	0.08 0.18
- 1598	0.04 0.20	0.06 0.24	-0.01 0.18
E230H- 1763	-0.20 0.19	-0.08 0.22	0.19 0.16
- 1963	0.03 0.32	0.04 0.29	0.04 0.25
- 2713	0.03 0.11	0.11 0.16	0.09 0.15